JOURNAL OF MATERIALS SCIENCE 19 (1984) 428–438

Lamellar crystallization of pendant chains in radiation-crosslinked polyethylene fibres

J. DE BOER, P. F. VAN HUTTEN, A. J. PENNINGS
Department of Polymer Chemistry, State University of Groningen, Nijenborgh 16, 9747 AG Groningen, The Netherlands

Ultra-high molecular weight polyethylene fibres of the gel-spun/hot-drawn type were crosslinked by means of γ-radiation and several techniques were applied for the characterization of the molecular network. The crosslinked fibres showed a nonperiodic morphology both in scanning EM and in SAXS. After a heat treatment above 150° C, the temperature at which the chain-extended crystals melt or transform into the hexagonal phase, a well-defined lamellar morphology was observed. This is ascribed to fast relaxation of pendant chains from the chain-extended crystals into a more kinked state, and subsequent lamellar crystallization of these chains upon cooling. From a determination of the amount of lamellar crystals it is estimated that about 90% of the network consisted of pendant chains, as a result of chain-scission during irradiation.

1. Introduction

Ultra-high strength polyethylene fibres, produced by the gel-spinning/hot-drawing technique [1, 2], contain a minimum amount of topological defects such as entanglements and loops. Accordingly, crosslinking of this material will result in networks with a reduced number of so-called network defects. These networks, therefore, should be especially suitable for experimental studies which are intended to verify recent developments of rubber-like elasticity theories [3–8] and of oriented crystallization [9–11].

Crosslinking ultra-high strength polyethylene filaments, without destroying the specific fibre structure, can only be performed using high-energy radiation, such as ^{60}Co γ-radiation. Unfortunately, apart from crosslinking, high-energy radiation causes main-chain scission [12, 13]. This implies that such networks can have a large number of dangling-chain irregularities, arising from chain scissions occurring in the course of crosslinking [14]. These dangling-chain irregularities are elastically inactive and do not contribute to the cycle rank [15] of the network. Furthermore, because of the randomness of the crosslinking process, these pendant chains are very likely to be branched.

In spite of the obvious importance of these dangling or pendant chains, relatively little has been done to characterize their effect on elastomeric properties. Part of the problem is to obtain information on the number and size of such irregularities in the network under consideration. In the present paper we demonstrate the presence of pendant chains in networks obtained by means of ^{60}Co γ-irradiation of ultra-high strength polyethylene fibres. Measurements on the melting behaviour of constrained crosslinked filaments indicate that about 90% of the network consists of pendant chains. It is shown by small angle X-ray scattering (SAXS) and by scanning electron microscopy (SEM) that upon constrained melting of the networks, the pendant chains can reorganize in such a way that during subsequent crystallization lamella-like crystals with a long period of 40 nm are obtained.

2. Experimental details

The polyethylene fibres used in this study were prepared from linear, ultra-high molecular weight polyethylene Hifax 1900 (from Hercules, $M_w \approx 4 \times 10^6$ kg kmol^{-1}). A filament was produced by extruding a 5 wt% solution of the polymer in paraffin oil at 170° C. After extraction of paraffin oil, the filament was drawn to a ratio of 24 at

0022–2461/84 $03.00 + .12

150° C. Experimental details have been reported previously [1, 2].

The drawn fibre was wound and fixed on a glass cylinder and contained in an evacuated glass cell. In this cell it was annealed for 64 h at 140° C in order to eliminate stress concentrations. Subsequently, the cell was irradiated by ^{60}Co γ-radiation at room temperature up to an effective dose of 86 kGy. Annealing at 140° C for 2 h was carried out afterwards in order to eliminate trapped free radicals. A more detailed description of the procedure was recently published [13, 16]. No extraction of sol fraction was made prior to the experiments described in this paper. The gel content was determined later and was found to be 84%.

In this paper, the thermal properties of radiation-crosslinked fibres will be compared with those of fibres, obtained by crosslinking ultra-high molecular weight polyethylene in the oriented state with dicumylperoxide. Details of this latter procedure will be described in a forthcoming paper [17].

Phase transition temperatures and associated heat effects were measured by means of a Perkin Elmer DSC-2 equipped with a Scanning Autozero Unit. Indium was used for the calibration of both the temperature scale and the heats of fusion at the scan speed used, which amounted to 10 K min^{-1}. The heats of fusion are expressed in kJ per kg of total polymer sample. In order to keep the networks extended while in the melt, the fibre was wound on a square 4 mm x 4 mm aluminium frame and knotted at the ends. The free ends of the fibre were cut off. Cooling between scans was carried out at −40 K min^{-1}.

Small-angle X-ray scattering curves were recorded by means of a Kratky camera with stepscanning device. Cu$K\alpha$ radiation was produced by a Philips PW 1130 generator operated at 45 kV and 45 mA. A nickel-filter and pulse-height discrimination were employed for monochromatization. Meridional slit-smeared scattering curves were recorded from a fibre which was uniformly wound on a rectangular sample frame in such a way that the fibre axis was perpendicular to the plane of the X-ray beam, The latter has a line-shaped cross-section. The sample frame was contained in an evacuated heating cell which allows measurements at high temperatures. The temperature was continuously monitored by means of a thermocouple near the sample, and it was kept constant to within 1° C by an electronic device (Knauer, Berlin) coupled with a Pt-100 resistor in the cell. The recording of one SAXS curve required about 1 h, in which 31 points were measured (up to 0.12 nm^{-1}). No corrections for parasitic and air scattering were made.

Scanning electron micrographs (SEM) were taken in an ISI DS-130 microscope operated at 40 kV, from gold-covered samples.

3. Results and discussion

3.1. Fibre-network formation

A fibre was produced by gel spinning of ultra-high molecular weight polyethylene followed by hot-drawing of the spun filament to a ratio of 24 at 150° C. The tensile strength of the drawn fibre amounted to 1.6 GPa. The fibre was subsequently crosslinked by γ-irradiation (86 kGy dose).

In order to clarify our interpretation of experimental results, we will first give a description of the mechanism of fibre and network formation. During the spinning process the gel of entangled molecules becomes inhomogeneous and breaks up into flow units as a result of elastic forces [18, 19]. Such a flow unit is a long bundle of partly extended molecules, in which regions of close-packed parallel arrangement alternate with droplet-like disordered domains containing the entanglements as well as loops and cilia. From the regions of extended and parallel chains, fibril backbones are formed upon crystallization. Loops and cilia will give rise to the growth of lamellar crystals epitaxially deposited on the backbone ("shish-kebabs").

Fibres with a tensile strength up to 4.1 GPa can be obtained from gel-spun filaments by means of hot-drawing in the temperature range 135 to 150° C. This process of further chain extension relies on the presence of chain loops and cilia emerging from entanglement sites. Although the chain mobility in the disordered regions is high and the lamellar crystals are molten above 135° C, the life-time of entanglements is very long at temperatures below 150° C since they are trapped between the adjacent chain-extended crystals. Conversely, these orthorhombic crystal blocks are stress-stabilized and prevented from "peeling off" by the entanglements at the end surfaces [20]. At 150° C, however, orthorhombic crystals are no longer stable and transform into the hexagonal phase [21], in which the chains can easily slide past each other. Above this temperature entangle-

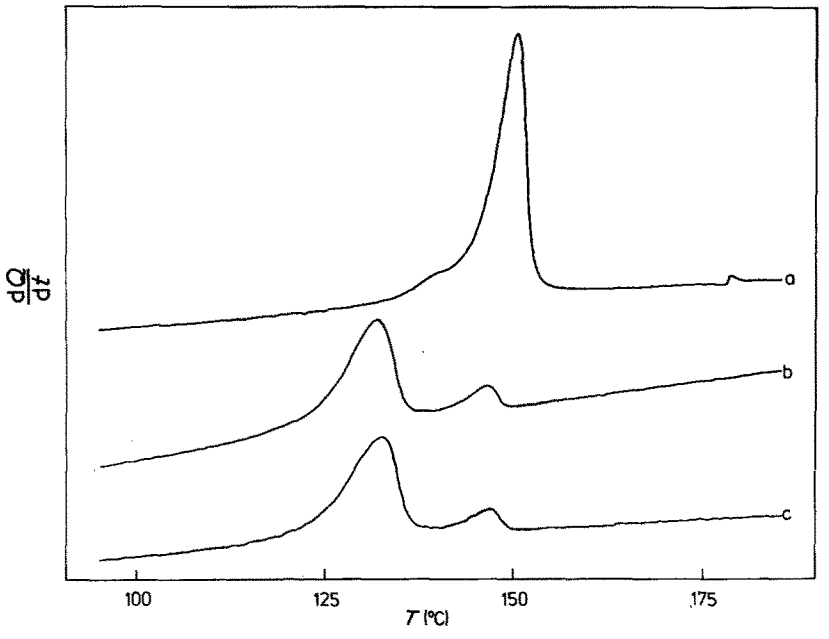

Figure 1 DSC thermograms of the radiation-crosslinked polyethylene fibre, recorded during constrained heating at a rate of 10 K min^{-1}. (a) first scan, directly after crosslinking; (b) second scan of the same sample; (c) third scan. The cooling rate between scans was 40 K min^{-1}.

ment life-times are too short for drawing to be effective. During hot-drawing the chain loops and cilia are converted into straight stems which add to the length of the chain-extended blocks. A further accumulation of entanglements in disordered zones occurs, while some entanglements slip off. Previous results have already shown that in a fibre drawn to a ratio of 24 the chains are not yet fully extended [2], and longer chains will still be involved in several entanglements.

γ-Irradiation of such a drawn fibre will lead to crosslink formation and chain fracture both occurring primarily in the disordered regions. Whereas radical recombination may follow chain fracture in the crystal lattice, fractured taut tie-molecules in the disordered zones will immediately contract. In this way chain ends and considerable branching will be introduced. A reduction in tensile modulus and strength upon γ-irradiation is consistent with this picture and was experimentally found [13].

3.2. Differential scanning calorimetry (DSC) and scanning electron microscopy

In order to characterize the complex molecular topology of the crosslinked fibre, it was examined by means of DSC. The fibre was wound on an aluminium frame so as to achieve constrained melting.

Three successive heating scans conducted on the same sample are presented by the thermograms of Fig. 1. The peak temperatures and the heats of fusion measured at a heating rate of 10 K min^{-1} are summarized in Table I. Curve a in Fig. 1 represents the behaviour of the fibre directly after the crosslinking procedure. The first endothermic effect appears as a very weak shoulder around 140° C. It can be ascribed to the melting of a lamellar chain-folded phase. The temperature is relatively high, but this can be accounted for by the presence of severe constraints on the chains in the lamellae. A broad range of melting tempera-

TABLE I Peak temperatures and heats of fusion of a constrained molten crosslinked fibre. The fibre was γ-irradiated with a dose of 86 kGy. It was scanned in DSC (see Fig. 1) prior to extraction of the sol fraction

	T_{m_1} (° C)	T_{m_2} (° C)	T_{m_3} (° C)	ΔH_1 (kJ kg^{-1})	ΔH_2 (kJ kg^{-1})	ΔH_3 (kJ kg^{-1})
First scan, a	(139.5)	149.8	177.9	–	192.4	1.4
Second scan, b	132.8	146.3	–	99.5	13.1	–
Third scan, c	133.0	147.0	–	100.8	11.4	–

tures for the lamellar phase was also found in surface-growth fibres [22, 23]. The second, main peak is found at 149.8° C. This endotherm is attributed to the solid-solid phase transition taking place in the chain-extended crystals. The orthorhombic crystal structure transforms into the hexagonal crystal modification. Those crystals in which the chains cannot relax because they are constrained by crosslinks or long-lived entanglements, remain in the hexagonal phase, while unconstrained crystals melt completely. This orthorhombic–hexagonal transition was found in various surface-growth and gel-spun fibres [22, 24]. The final, small effect at 178° C in the first DSC scan might be due to retarded melting of some of the hexagonal crystals [22, 25].

After cooling down to room temperature at a rate of $40\,K\,min^{-1}$, a second heating scan was carried out. This second scan, curve b in Fig. 1, is completely different from the first scan. A similar phenomenon was observed during constrained melting of γ-irradiated surface-growth fibres [24]. The first and strongest endothermic peak appears at 132.8° C. This corresponds to the melting of lamellar crystals composed of chains with few conformational constraints. At 146.3° C, the transition of the chain-extended crystals is found, but the endothermic effect is much weaker than in the first scan. The changes in the DSC pattern indicate a drastic decrease in the amount of chain-extended crystals as a result of heating above the transition temperature of 150° C during the first scan. As a consequence of the relaxation of many extended chains, a much larger amount of lamellar crystals than originally present, has been formed upon cooling. The third DSC scan, curve c, is equal to the second one, which means that no further reorganization has taken place during the second heating cycle. The reproducibility of the endotherm at 146 to 147° C suggests that it pertains to the reversible orthorhombic–hexagonal transition of persistent chain-extended crystals.

One might calculate the weight fractions of polyethylene involved in the transition of the orthorhombic crystals into the hexagonal phase or the melt from the DSC scans and the values for the enthalpy change of these transitions. A first estimate may be found in the values known for similar transitions in the odd-numbered *n*-paraffins [26], which amount to approximately 90 and $150\,kJ\,kg^{-1}$ for the orthorhombic–hexagonal and hexagonal–melt transition, respectively. Results obtained in our laboratory [27], however, have shown that for constrained melting of polyethylene fibres, the heats of transition approach constant values at very high draw ratios, approximately 190 and $55\,kJ\,kg^{-1}$ for the orthorhombic–hexagonal and hexagonal–melt endotherm, respectively. If our data on polyethylene are assumed to be representative for chain-extended crystals in which the chains are constrained, they indicate that the hexagonal phase in polyethylene is closer to the melt state than expected from similar transitions in *n*-paraffins. For the odd-numbered paraffins, it should be noted indeed, the heat value for the orthorhombic–hexagonal transition increases with the chain length (and therefore with increasing transition temperature), while that of the hexagonal–melt transition decreases. This is in line with the difference between the values found for polyethylene and those for paraffins. When one applies our value of $190\,kJ\,kg^{-1}$ to the reversible orthorhombic–hexagonal peak in the second DSC scan, it is calculated that 7 wt % of the crosslinked polyethylene is contained within those chain-extended crystals. After the first heating cycle, therefore, 93% of the fibre consists of lamellae or more disordered regions. If one assumes that the sol fraction of 16 wt % is to be found exclusively in the lamellae, a correction for the sol fraction can be carried out and one finds that 92% of the network has recrystallized into a chain-folded phase. A discussion of these results will be given in Section 3.4. It should be mentioned that after this DSC experiment, the fibre was still taut around the sample frame. The implications of this finding will also be discussed later.

Figs. 2 and 3 show SEM micrographs of the fibre before and after the DSC treatment. Whereas the initial morphology is irregular, a very distinct structure of well-aligned and intermeshed lamellae can be observed on the sample surface after the DSC experiment. The maximum lamellar thickness including one boundary layer is approximately 46 nm; the number average long period amounts to 39 nm.

3.3. Small-angle X-ray scattering and X-ray diffraction

Meridional SAXS curves recorded in the course of various heat treatments are shown in Figs. 4 and 5. The same fibre sample was used through-

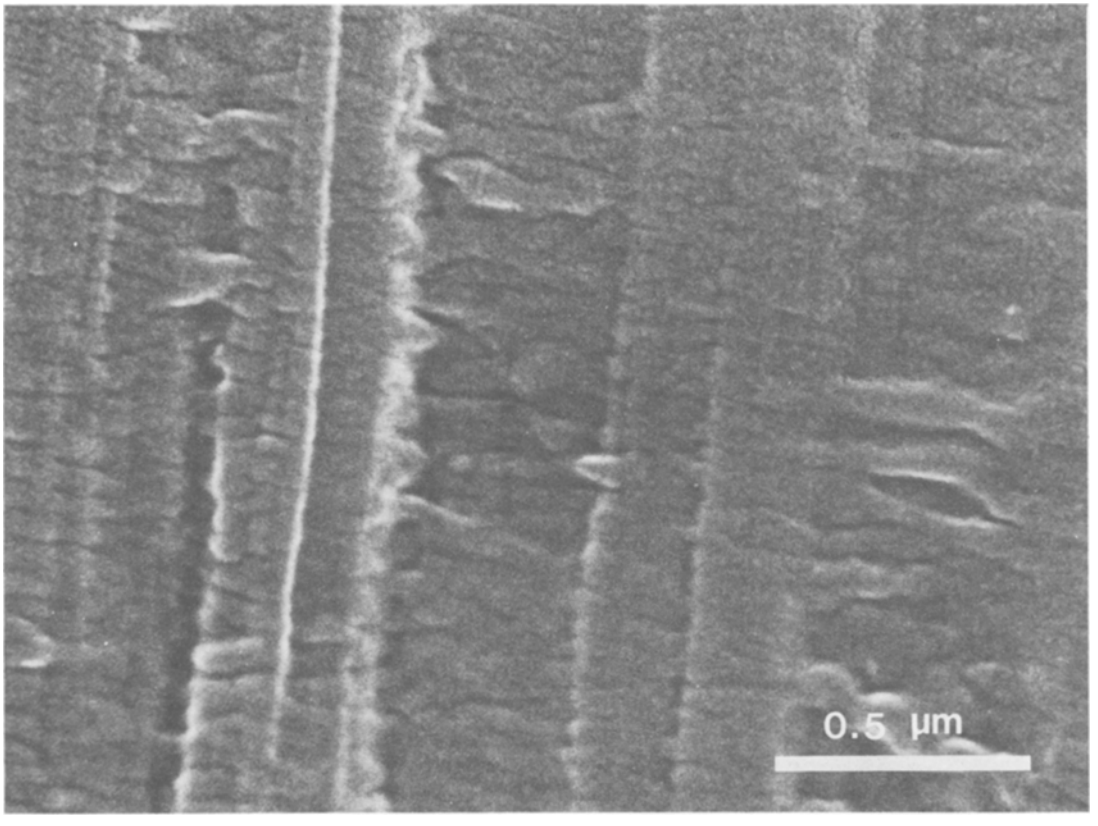

Figure 2 Scanning electron micrograph of the radiation-crosslinked polyethylene fibre which was the starting material for the experiments described. The surface morphology is highly irregular.

out. In Fig. 4, curve A represents the scattering from the intitial sample. There is no indication of a long period in the angular region covered, which ranges from $(85\,\text{nm})^{-1}$ to $(9\,\text{nm})^{-1}$, although the sample was annealed for 2 h at 140° C after irradiation.

The sample was heated in the SAXS set-up to a maximum temperature of 142° C and curve B was recorded. The intensity at 142° C was somewhat higher than at 25° C. Since the presence of lamellar material would result in an intensity reduction due to melting around 140° C [23], SAXS indicates that the amount of distinctly lamellar phase must have been very small. This is in line with the DSC result, curve a in Fig. 1. The sample was left to cool down to room temperature; the cooling rate amounted to approximately $10\,\text{K}\,\text{min}^{-1}$ in the crystallization range. At room temperature curve C was found. The intensity is higher than before and shows a very faint shoulder at $b \approx 0.02\,\text{nm}^{-1}$. (This shoulder was observed more clearly at higher temperatures, which is due to reversible changes in the disordered regions with temperature.)

The first heating and cooling cycle has obviously resulted in a limited formation of lamellar structures. It may well be that only the surface of the elementary fibrils has been affected. A second heating cycle was undertaken and SAXS curves were recorded at various temperatures. After a strong initial rise, a decrease in intensity was already observed around 130° C. At 142° C the SAXS was found to level off and to become almost equal to that in the first scan (curve B), but a substantial further decrease was observed upon heating to 150° C (curve D). After cooling to room temperature curve E was recorded. A broad peak appears, the maximum of which corresponds to a long period of 44 nm. In agreement with the DSC results, the orthorhombic–hexagonal transition and the concomitant relaxation of chain-extended material has taken place at 150° C, and as a result a pronounced lamellar morphology has formed upon cooling.

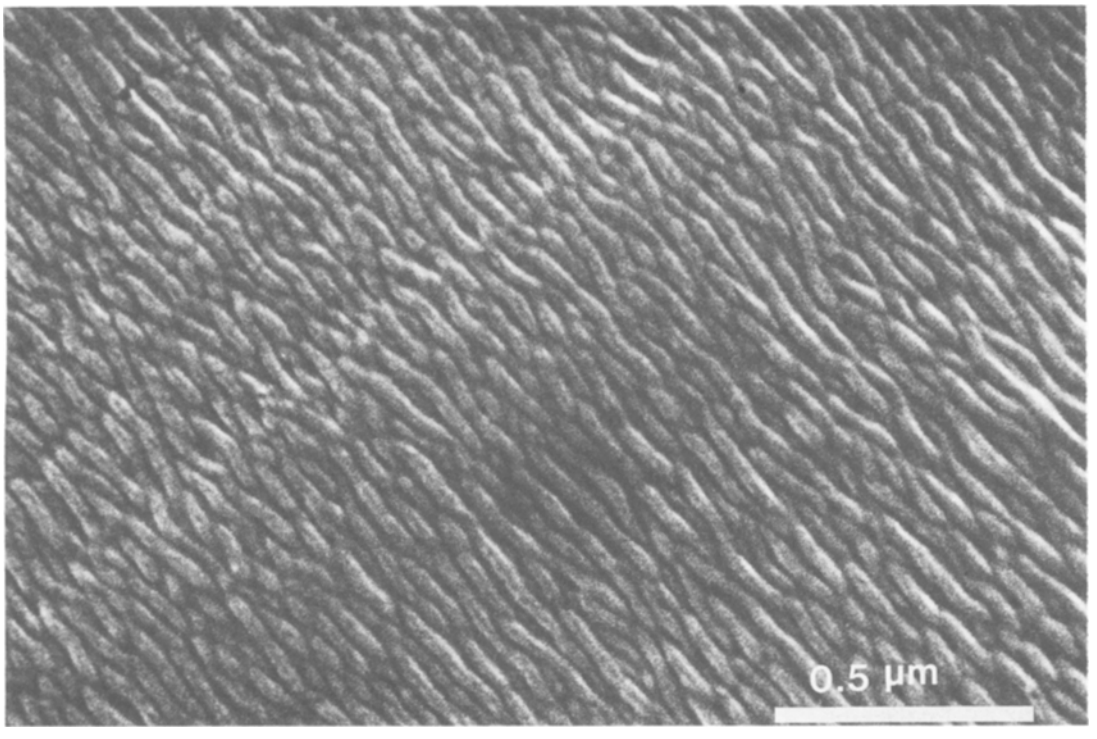

Figure 3 Scanning electron micrograph of the radiation-crosslinked polyethylene fibre after having been subjected to the DSC experiment of Fig. 1. A well oriented and space-filling lamellar morphology is visible.

A third cycle was carried out in the SAXS set-up in order to explore the influence of crystallization conditions (Fig. 5). Upon heating, the intensity of the 44 nm maximum increased strongly and above 100° C it shifted towards smaller angles. This was followed by a decrease in intensity over the whole angular range covered when the temperature was raised above 130° C. This behaviour can be fully understood from the DSC curve b in Fig. 1, which indicates that the lamellar phase melts over a broad temperature range below 135° C. At 142° C curve A in Fig. 5 was recorded (note that Figs. 4 and 5 have different scales). In this experiment, the fibre was

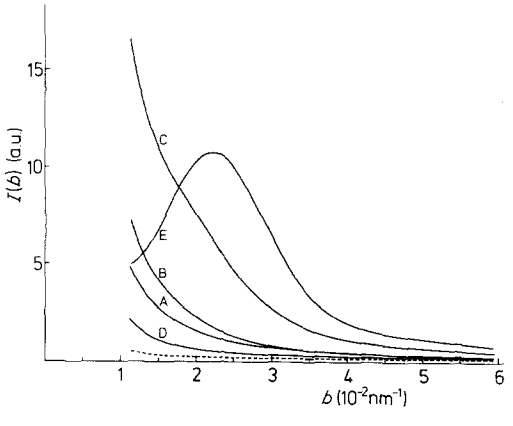

Figure 4 Slit-smeared meridional SAXS curves of the radiation-crosslinked polyethylene fibre, recorded successively at various temperatures during constrained heating. First cycle: (A) 25° C; (B) 142° C; (C) 25° C. Second cycle: (D) 150° C; (E) 25° C. The dashed line indicates the blank scattering at 25° C. b is the reduced scattering angle $2 \sin\theta/\lambda$.

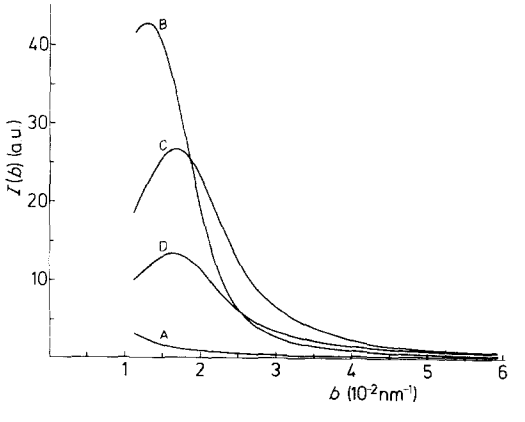

Figure 5 Slit-smeared meridional SAXS curves of the radiation-crosslinked polyethylene fibre. This figure is the continuation of Fig. 4. Third cycle: (A) 142° C; (B) 128° C after 22 h of crystallization at this temperature; (C) 100° C; (D) 25° C. $b = 2 \sin\theta/\lambda$.

cooled at a rate of 1 K min^{-1} from 142 to 128° C, and kept at 128° C for crystallization. After 22 h at 128° C, curve B in Fig. 5 was recorded. After rapid further cooling to 100° C curve C was found. The peak intensity decreased and its position shifted from 78 to 60 nm. This behaviour appeared to be reversible upon fast heating and cooling between 128 and 100° C. It can be explained by the mechanism of lateral lamellar growth between splayed lamellae, as discribed by Strobl *et al.* [28]. The micrograph of Fig. 3 shows lamellar splaying, and such a mechanism might be well possible in an oriented system.

The very high long period of 78 nm at 128° C can be accounted for by a crystallization process which starts with the secondary nucleation of very long stems on chain-extended substrates. The nature of these nucleation sites will be discussed in the next section. Further growth is characterized by a decrease in stem length and, therefore, by tapered and intermeshed lamellae. The chain-extended fibrils are covered by an extensive overgrowth of lamellar crystals and for this reason stem lengths as large as 78 nm are not observed on the surface micrograph of Fig. 3. Concomitantly, the SAXS long period will be systematically higher than the one calculated from SEM micrographs.

Further cooling of the fibre from 100° C to room temperature did not change the long period but merely reduced the intensity. This shows that no substantial lateral growth occurs below 100° C. The intensity decrease can be explained by an increase in the chain density in the defect regions between the lamellae, as well as to a reduction of the size of these regions [23]. The final long period is 60 nm instead of the 44 nm found upon rapid cooling. This crystallization experiment shows that the long period depends on the crystallization conditions.

Fig. 6 shows the X-ray diffraction pattern of the starting fibre at room temperature. The diffraction pattern of a fibre at constant length at approximately 160° C is reproduced in Fig. 7. It shows a diffuse "halo" from the melt and on the equator a single reflection, which stems from the hexagonal phase ($d = 0.44$ nm). The fibre which was heat treated in the SAXS set-up gave the diffraction pattern of Fig. 8, at room temperature. A minor increase in the arcing of the whole pattern, as compared to Fig. 6, indicates that the constraints on the fibre have been effective in preserving the orientation in most of the fibre.

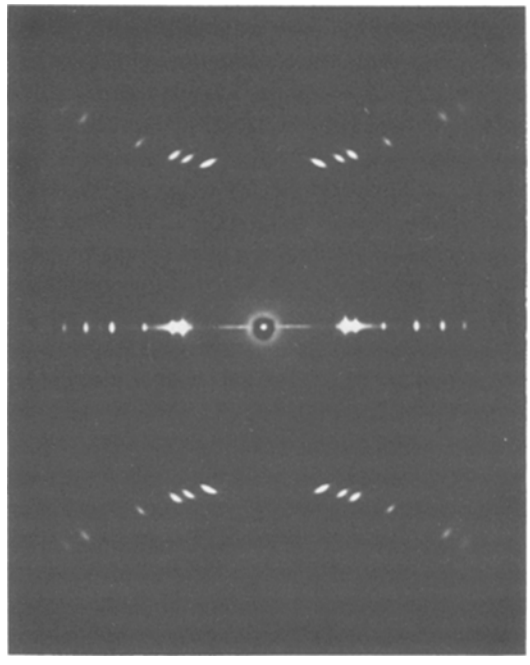

Figure 6 Wide-angle X-ray diffraction (WAXD) pattern of the radiation-crosslinked polyethylene fibre at room temperature. Fibre axis vertical.

Like in the DSC experiments, the macro-fibre was found to have remained taut around the sample frame after the treatment in the SAXS set-up. A weak ring emerging from the strongest reflections on the equator represents a small amount of material which has become disoriented.

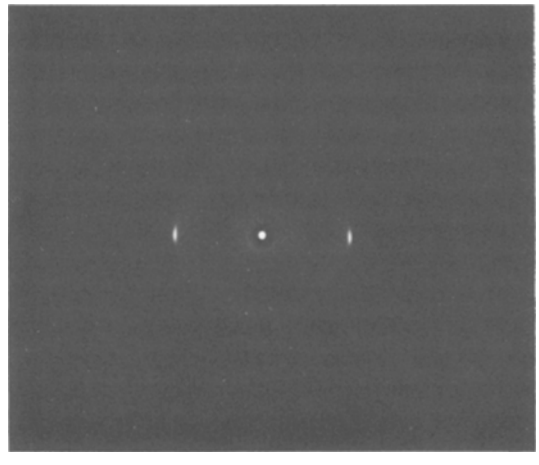

Figure 7 WAXD pattern of the radiation-crosslinked polyethylene fibre at approximately 160° C at fixed length. The discrete reflection stems from the hexagonal phase. Fibre axis vertical.

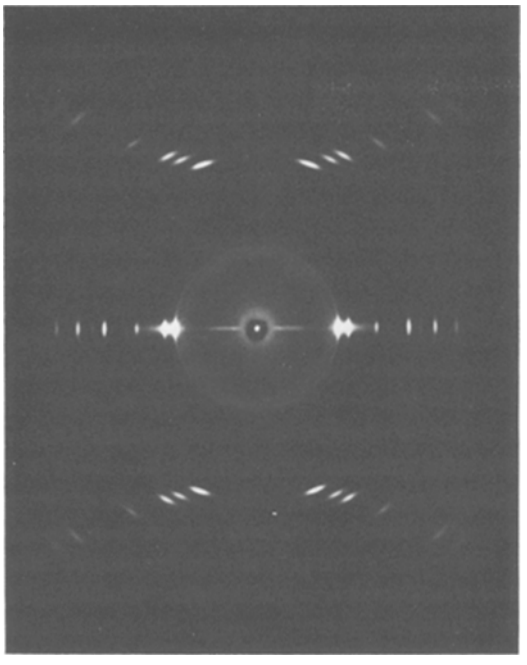

Figure 8 WAXD pattern of the radiation-crosslinked polyethylene fibre after having been used for the SAXS experiments of Figs. 4 and 5, in which a maximum temperature of 150° C was attained. Fibre axis vertical.

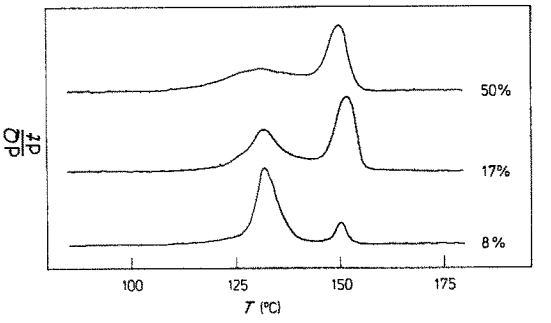

Figure 9 DSC thermograms of polyethylene fibres crosslinked in the oriented state with 8, 17 and 50 wt % of dicumylperoxide, respectively. Each fibre had received a heat treatment at 180° C at constant length prior to the DSC experiment.

3.4. Discussion of molecular mechanisms

An important observation is that the fibres remained taut on the sample frame during the heat treatment. This is in contrast to the behaviour of noncrosslinked fibres, which were found to have become longer upon heat treatments even when kept below the melting temperature. This elongation is due to chain slip occurring under the influence of strong retractive forces originating from the noncrystalline regions at high temperature. In the γ-irradiated fibres no length increase is found, which implies that there are continuous chain paths, constituting the cycle rank of the network, along the macroscopic sample as a result of crosslinking. It is therefore very likely that the elastically effective chains remain extended at all temperatures, and that the chains, which reorganize at 150° C, are not elastically effective. We believe that we are dealing with the relaxation of polymer chains which are anchored in the network with one end only, the so-called pendant chains. These pendant chains correspond partly to the initial chain-ends, but a much larger amount is formed as a result of main-chain scission during the irradiation procedure [13].

If pendant chains are indeed the chains that will rearrange from chain-extended crystals to lamellae upon constrained heating and cooling, such a rearrangement should be absent in the case of densely crosslinked fibres. In the latter, the mass of pendant chains is relatively low, which implies that practically all chains should remain extended during constrained melting of such networks. Densely crosslinked fibre networks were produced by vulcanizing as-spun polyethylene fibres in the oriented state with dicumylperoxide [17], which is known to crosslink polyethylene without chain fracture [29]. Fig. 9 represents DSC thermograms of fibres crosslinked in this way with 8, 17 and 50 wt % dicumylperoxide. The thermograms were obtained after the fibres had been heated to 180° C and subsequently crystallized at constant length. Fig. 9 shows that the ratio of the surface area under the endotherm at 130° C to the surface area of the peak at 150° C decreases with increasing dicumylperoxide content. Obviously, a higher degree of crosslinking is accompanied by a reduced extent of rearrangement upon constrained melting. This observation supports the idea that the pendant chains in the network are responsible for the reorganization effect, since their mass diminishes with increasing crosslink density.

From the similarity of the second and third DSC scan of the γ-irradiated fibres (Fig. 1) it may be concluded that the relaxation at 150° C proceeds very rapidly. This implies that no long-range reptational motion of the pendant chains is involved, since lateral reptation of a chain is the very viscous melt is an extremely slow process [30]. Moreover, pendant chains are likely to be branched, which further reduces their mobility. The only probable motion of a pendant chain

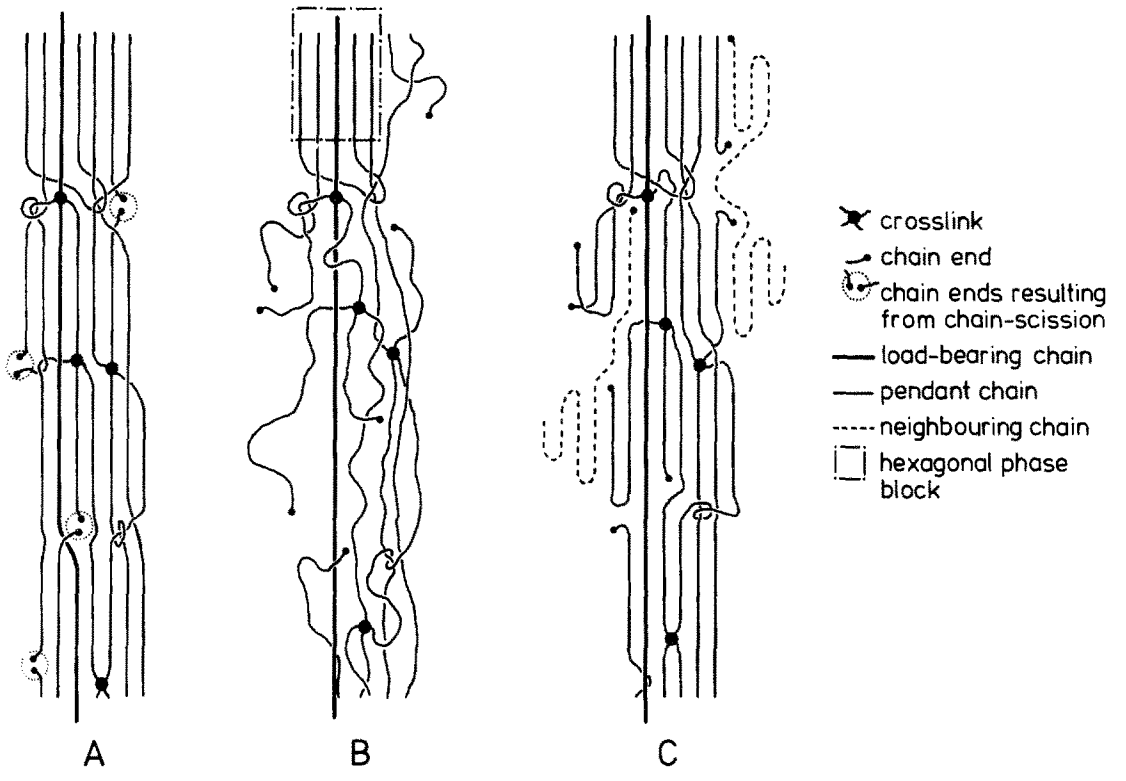

Figure 10 Schematic drawing of the molecular topology of the fibre-network in various stages. (A) After crosslinking in the solid state, crosslinks and chain-ends resulting from chain-scissions are to be found in the disordered regions between chain-extended crystallites. (B) Above 150° C orthorhombic crystallites have transformed into the hexagonal phase and some contraction of extended pendant chains has taken place. A small fraction of chains is permanently under tension. Hexagonal crystallites are preserved as a result of conformational constraints. (C) After the heat treatment lamellae have formed. The load-bearing chain has acted as a nucleus for long-stem crystallization. A decrease in stem length has resulted in tapered lamellae.

upon melting of the chain-extended crystals will be a longitudinal contraction as a result of entropy forces. This contraction will be sufficient so as to introduce kinks in the chain and make it look like a succession of blobs [30]. On the whole, the chain will be confined within its "tube" of approximately 3 nm diameter [31], and its overall conformation along the fibre axis will be preserved. As a consequence of the limited mobility of pendant chains, due to entanglements and branches, their crystallization may proceed like in the "solidification" model [32], which corresponds to regime III crystallization [33].

According to the calculation presented in Section 3.2, the lamellar crystals formed after heat treatment at 150° C constitute approximately 90% of the material, which suggests that the γ-irradiated fibre contains a large amount of pendant chains. In order to evaluate this result, it is pertinent to discuss the molecular topology of the radiation-crosslinked fibre. In view of the strong rearrangement effects observed we expect that the number density of elastically effective network chains will be low. Since these chains will be under tension permanently, they are not likely to assemble and form a bundle-like nucleus upon crystallization. Instead, each of these low-entropy chains may act as a substrate and induce oriented crystallization of surrounding chains at relatively high temperatures (Fig. 10). The initial sequences may crystallize with a very high stem length. On one hand, this picture implies that a number of elastically ineffective chains will participate in the formation of crystals of chain-extended character. The endotherm at 146° C found in the second and further DSC scans, therefore, cannot be entirely attributed to constrained network chains. On the other hand, the dispersed state of the elastically effective network chains will seriously restrict the diameter of the chain-

extended crystals that they induce. Since the reptation rate of branched pendant chains is low, further growth of chain-extended crystals is hampered. Consequently, crystallization will be characterized by a decreasing stem length and a decrease in temperature. The chain-extended core of the crystals thus formed will be very thin and it will have a high surface free energy. In view of this, the value of 190 kJ kg^{-1}, which was obtained from highly drawn fibres, will be too high for the orthorhombic–hexagonal transition of these core crystals and will lead to an underestimation of the amount of crystal phase which melts at 146° C.

It is impossible at this moment to quantify the influence of these opposing factors on the determination of the number of elastically effective, permanently constrained chains. At this stage we will neglect these factors and simply attribute the endotherms at 146° C to a reversible orthorhombic–hexagonal transition of permanent chain-extended crystals. This implies that the lamellar phase roughly represents the amount of pendant chains and loose chains. According to the previous calculations, therefore, 92 wt % of the polyethylene network might be formed by pendant chains.

The process of orientation-induced crystallization on constrained chains as described above, will explain the very long SAXS period measured at high temperatures. In order to explain the temperature dependence of the SAXS peak intensity, which is similar to that found for the heat treated shish-kebab type overgrowth [23], the occurrence of density gaps at the lamellar surfaces must be considered. Chain ends will contribute, but chain backfolding will also play a role. It will be very interesting to study the chain conformation in more detail, since the abundance of pendant chains will have a strong influence on the elastic properties of the network in the rubbery state. This point will be the subject of future publications [34].

Acknowledgements

The authors would like to thank H. -J. van den Berg for his assistance in the crosslinking experiments and B. A. Klazema for his help in the SEM work. The authors are furthermore indebted to J. Smook for supplying the gel-spun/hot-drawn fibres, melting data, and for many stimulating discussions.

This study was supported by the Netherlands Foundation for Chemical research (SON) with financial aid from the Netherlands Organization for the Advancement of Pure Research (ZWO).

References

1. B. KALB and A. J. PENNINGS, *J. Mater. Sci.* **15** (1980) 2584.
2. J. SMOOK, M. FLINTERMAN and A. J. PENNINGS, *Polym. Bull.* **2** (1980) 775.
3. G. RONCA and G. ALLEGRA, *J. Chem. Phys.* **63** (1975) 4990.
4. P. J. FLORY, *Proc. Roy. Soc. Lond.* **A351** (1976) 351.
5. *Idem, J. Chem. Phys.* **66** (1977) 5720.
6. L. M. DOSSIN and W. W. GRAESSLEY, *Macromolecules* **12** (1979) 123.
7. H. -G. KILIAN, *Polymer* **22** (1981) 209.
8. P. J. FLORY and B. ERMAN, *Macromolecules* **15** (1982) 800.
9. R. J. GAYLORD, *J. Polym. Sci. Polym. Phys. Ed.* **14** (1976) 1827.
10. A. POSTHUMA DE BOER and A. J. PENNINGS, *Faraday Disc. Chem. Soc.* **68** (1979) 345.
11. K. J. SMITH Jr, in "Elastomers and Rubber Elasticity", edited by J. E. Mark and J. Lal, ACS Symposium Series, No. 193 (ACS, Washington DC, 1982) Chap. 15, p. 293.
12. G. UNGAR and A. KELLER, *Polymer* **21** (1980) 1273.
13. J. DE BOER and A. J. PENNINGS, *Polym. Bull.* **5** (1981) 317.
14. A. L. ANDRADY. M. A. LLORENTE, M. A. SHARAF, R. R. RAHALKAR, J. E. MARK, J. L. SULLIVAN, C. U. YU and J. R. FALENDER, *J. Appl. Polym. Sci.* **26** (1981) 1829.
15. J. A. DUISER and A. J. STAVERMAN, in "Physics of Non-Crystalline Solids" (North-Holland Publishing Co., Amsterdam, 1965) p. 376.
16. J. DE BOER and A. J. PENNINGS, *Polym. Bull.* 7 (1981) 309.
17. J. DE BOER, H. -J. VAN DEN BERG and A. J. PENNINGS, *Polymer* in press.
18. J. SMOOK and A. J. PENNINGS, *Polym. Bull.* 9 (1983) 75.
19. *Idem, J. Mater. Sci.* **19** (1984) 31.
20. J. C. M. TORFS, G. O. R. ALBERDA VAN EKENSTEIN and A. J. PENNINGS, *Eur. Polym. J.* **17** (1981) 157.
21. J. SMOOK, J. C. M. TORFS and A. J. PENNINGS, *Makromol. Chem.* **182** (1981) 3351.
22. A. J. PENNINGS and A. ZWIJNENBURG, *J. Polym. Sci. Polym. Phys. Ed.* **17** (1979) 1011.
23. P. F. VAN HUTTEN, A. J. PENNINGS and A. M. KIEL, *J. Mater. Sci.* **17** (1982) 3525.
24. J. C. M. TORFS, "Ultra-Strong Polyethylene Fibers Produced by Crystallization from Flowing Solutions", PhD thesis, Groningen (1983) p. 137.
25. A. J. PENNINGS and J. M. A. A. VAN DER MARK, *Rheol. Acta* **10** (1971) 174.
26. A. A. SCHAERER, G. G. BAYLE and W. M. MAZEE, *Recueil Trav. Chim. Pays-Bas* **75** (1956) 529.
27. J. SMOOK and A. J. PENNINGS, to be published.
28. G. R. STROBL, M. J. SCHNEIDER and I. G. VOIGT-MARTIN, *J. Polym. Sci. Polym. Phys. Ed.* **18** (1980) 1361.

29. A. POSTHUMA DE BOER and A. J. PENNINGS, *J. Polym. Sci. Polym. Phys. Ed.* **14** (1976) 187.
30. P.-G. DE GENNES, "Scaling Concepts in Polymer Physics" (Cornell University Press, Ithaca, 1979) Chap. 8.
31. W. W. GRAESSLEY, *J. Polym. Sci. Polym. Phys. Ed.* **18** (1980) 27.
32. E. W. FISCHER, *Pure Appl. Chem.* **50** (1978) 1319.
33. J. D. HOFFMAN, *Polymer* **24** (1983) 3.
34. J. DE BOER and A. J. PENNINGS, *Colloid Polym. Sci.* **261** (1983) 750.

Received 13 May
and accepted 26 May 1983